

ADVANCED MATERIALS

Supporting Information

for *Adv. Mater.*, DOI 10.1002/adma.202311498

Glucose-Triggered Gelation of Supramolecular Peptide Nanocoils with Glucose-Binding Motifs

*Sihan Yu, Zhou Ye, Rajdip Roy, Ravi R. Sonani, Irawan Pramudya, Sijie Xian, Yuanhui Xiang, Guoqiang Liu, Belen Flores, Einat Nativ-Roth, Ronit Bitton, Edward H. Egelman and Matthew J. Webber**

Supporting Information

**Glucose-Triggered Gelation of Supramolecular Peptide Nanocoils with
Glucose-Binding Motifs**

Sihan Yu,^{#,1} Zhou Ye,^{#,1} Rajdip Roy,¹ Ravi R. Sonani,² Irawan Pramudya,¹ Sijie Xian,¹ Yuanhui Xiang,¹ Guoqiang Liu,³ Belen Flores,¹ Einat Nativ-Roth,⁴ Ronit Bitton,⁴ Edward H. Egelman,² and Matthew J. Webber^{1,*}

1- University of Notre Dame, Department of Chemical & Biomolecular Engineering, Notre Dame, IN 46556 USA

2- University of Virginia, Department of Biochemistry and Molecular Genetics, Charlottesville, VA 22903 USA

3- University of Notre Dame, Integrated Biomedical Sciences Program, Notre Dame, IN 46556 USA

4- Ben-Gurion University of the Negev, Department of Chemical Engineering, Beer-Sheva, 84105, Israel

*- Correspondances addressed to: mwebber@nd.edu

[#]SY and ZY contributed equally to this work.

Contents:

Detailed Experimental Methods

Supplementary Data

- Figure S1-** PBA-MDP chemical structure
- Figure S2-** COOH-MDP chemical structure
- Figure S3-** OH-MDP chemical structure
- Figure S4-** TEM analysis of PBA-MDP over a range of glucose concentrations
- Figure S5-** TEM analysis of COOH-MDP
- Figure S6-** TEM analysis of OH-MDP
- Figure S7-** Rheology of COOH-MDP
- Figure S8-** Release profile of MCA-dasiglucagon alone
- Figure S9-** ESI-MS of PBA-RFVAAWVK
- Figure S10-** Analytical HPLC of PBA-RFVAAWVK
- Figure S11-** ESI-MS of COOH-RFVAAWVK
- Figure S12-** Analytical HPLC of COOH-RFVAAWVK
- Figure S13-** ESI-MS of OH-RFVAAWVK.
- Figure S14-** Analytical HPLC of OH-RFVAAWVK
- Figure S15-** ESI-MS of dasiglucagon
- Figure S16-** Analytical HPLC of dasiglucagon

Detailed Experimental Methods

1. Peptide Synthesis & Purification. All MDPs were synthesized by solid-phase methods using a CEM Liberty Blue synthesizer. Fmoc-protected amino acids and Rink amide resin (0.94 emq/g, 100-200 mesh) were purchased from ChemImpex. Coupling reactions were performed using diisopropylcarbodiimide (DIC) and Oxyma in DMF with microwave heating. At the N-terminal positions, peptides were modified on resin using 4-carboxyphenylboronic acid pinacol ester (PBA-MDP), 4-(tert-Butoxycarbonyl)benzoic acid (COOH-MDP), or 4-(tert-Butoxy)benzoic acid (OH-MDP) by hand using standard coupling methods. Completed peptides were cleaved from resin by treatment with trifluoroacetic acid (TFA)/triisopropylsilane/H₂O (95:2.5:2.5, v/v/v) for 2 h at room temperature. The cleavage liquid was then concentrated under a vacuum to remove most TFA and precipitated in cold diethyl ether. Crude material was collected by centrifugation, with excess ether being decanted and the remaining solid air-dried overnight. The crude peptide was then purified using by dissolving in hexafluoro-2-propanol (HFIP) at a concentration of 100–150 mg/mL and injecting onto a Biotage Isolera flash chromatography system using a reversed-phase bio-C₁₈ cartridge (25g) at a flow rate of 40 mL/min with a linear gradient from 0 to 100% (v/v) acetonitrile (+0.1% TFA) in water. Wavelengths of 220 and 280 nm were monitored for fraction collections, and collected fractions were then verified by electrospray ionization mass spectrometry (ESI-MS, Advion) and high-performance liquid chromatography (HPLC) using a C₁₈ Gemini (Phenomenex) column (*Fig S9-S14*). Fractions with verified purity were combined and lyophilized, yielding a slightly yellowish powder product. The synthesis of dasiglucagon (*Fig S15-S16*) and a fluorescent variant (MCA-dasiglucagon) was performed according to previous reports.^[1]

2. Preparation of MDP Samples. PBA-MDP was first dissolved in deionized (DI) water at a concentration of 3% (w/v) and adjusted to pH 7.4 using 0.1 M NaOH. Then an equal volume of 2x HEPES buffer (20 mM HEPES, 280 mM NaCl) containing different glucose concentrations was added for final glucose concentrations of 0, 25, 50, 100, 200 mg/dL and final peptide concentration of 1.5% (w/v). COOH-MDP and OH-MDP were prepared identically at a final glucose concentration of 0 mg/dL.

3. Fourier Transform Infrared Spectroscopy (FTIR) Samples were prepared as described in Section 2 and lyophilized overnight. The dried powder was then analyzed using a Jasco FT/IR-6300 spectrometer. A background of air was subtracted for all spectra.

4. Circular Dichroism (CD) Spectroscopy. CD was collected using a Jasco J-1700 instrument. PBA-MDP were first prepared as reported in Section 2 at 1.5% w/v and diluted immediately before measurement by 10 times with 5 mM HEPES buffer at varying glucose concentration for a final peptide concentration of 0.15% w/v and glucose concentrations of 0, 25, 50, 100, and 200 mg/dL. COOH-MDP and OH-MDP samples were prepared identically, with a final glucose concentration of 0 mg/dL. To collect spectra, 50 μ L of the diluted peptide solution was transferred to a quartz plate cuvette with a path length of 0.1 mm. Three spectra were collected (range of 250–190 nm, 50 nm/min scanning speed) and averaged for each sample. A background of 5 mM HEPES buffer was subtracted from all samples.

5. Small-angle X-ray Scattering. PBA-MDP samples prepared as noted in Section 2 at 1.5% w/v in HEPES buffer with a final glucose concentration of 0 or 100 mg/dL were subjected to small angle x-ray scattering with a SAXSLAB GANESHA 300-XL. CuK_α radiation was generated by a Genix 3D Cu-source with an integrated monochromator, 3-pinhole collimation and a two-dimensional Pilatus 300 K detector. The scattering intensity, q , was recorded at intervals of $0.012 < q < 0.3 \text{ \AA}^{-1}$ (corresponding to lengths of 10-800 \AA). Measurements were performed under vacuum at ambient temperature. The scattering curves were corrected for counting time and sample absorption. The PBA-MDP sample was sealed in thin-walled quartz capillaries about 1.5 mm in diameter and 0.01 mm wall thickness. The scattering spectra of the solvent were subtracted from the corresponding solution data using the Irena package for analysis of small-angle scattering data.^[2] Quantitative data analysis of KsEEKs was based on fitting its scattering curve to a model of spherical units packed into a helical structure,^[3] with aid from SASfit software.^[4] For complete details of this model, please refer to a prior report on its use to ascertain structure of related peptide nanocoil assemblies.^[5]

6. Transmission Electron Microscopy (TEM). Peptide samples were prepared at 1.5% w/v as described in Section 2 and diluted 5 times in HEPES buffer immediately before TEM sample preparation. TEM samples were prepared by depositing a volume of 3 μ L peptide solutions onto

plasma-treated copper grids with a carbon film (Ted Pella, 200 mesh) for 45 s. After wicking away excess fluid and allowing the grid to dry in air, negative staining was applied using 2% uranyl acetate. TEM visualization was performed at an accelerating voltage of 120 kV (JOEL 2011).

7. Cryogenic Transmission Electron Microscopy. TEM at cryogenic temperature (Cryo-TEM) was used for direct imaging of solutions and dispersions. Vitrified specimens were prepared on a copper grid coated with a perforated lacey carbon 300 mesh (Ted Pella Inc.). A 3 μ L drop from the solution was applied to the grid and blotted with filter paper to form a thin liquid film of solution. The blotted samples were immediately plunged into liquid ethane at its freezing point (-183°C). The procedure was performed automatically in the Plunger (Leica EM GP). The vitrified specimens were then transferred into liquid nitrogen for storage. The samples were studied using a FEI Talos F200C TEM, at 200 kV maintained at -180°C ; and images were recorded by FEI Ceta 16M camera ($4\text{k} \times 4\text{k}$ CMOS sensor) at low dose conditions, to minimize electron beam radiation damage.

8. Structural Cryo-EM. The nanocoil solution was applied on a holey carbon support grid (Quantifoil R 2/1 on 200 copper mesh). Excess sample was blotted away and the grid with a thin film of solution was plunge-frozen in liquid ethane (-180°C) using an EM GP Plunge Freezer (Leica). A total of 5286 cryo-EM micrographs were collected with defocus range of -2.2 to -1.2 μm on a 300 keV Titan Krios electron microscope having a K3 camera housed at the University of Virginia. Each recorded movie had an accumulated exposure time of approximately 50 electrons per square angstrom ($\sim 50 \text{ e}/\text{\AA}^2$), while the pixel size of the images was ~ 1.08 \AA . The data processing was performed in cryoSPARC (v4.2.1).^[6] Micrographs were preprocessed by ‘Patch Motion Correction’ and ‘Patch CTF Estimation’ jobs for motion correction and contrast transfer function (CTF) estimation, respectively. The nanocoil segments were picked manually by ‘manual picker’ from several micrographs to generate the initial template for further automated picking. The ‘Filament Tracer’ was used for automated picking from the whole dataset. A total of 1,244,857 particles were picked with raw pixel size and subjected to the ‘2D classification’ job to remove junk particles. The averaged power spectrum of the aligned nanocoil segments was generated by the job ‘Average Power Spectra’ while the 3D reconstruction was done by the ‘Helix Refine’ job with helical symmetry consisting of twist/rise

of 15.68°/5.12 Å imposed. The structure of PBA-MDP was predicted by AlphaFold,^[7] manually fit in the density using COOT,^[8] and used for the model-to-map fit representation.

9. Atomic Force Microscopy (AFM). AFM samples were prepared by depositing a drop of peptide solution (0.2% w/v in pH 7.4 HEPES buffer) on a mica surface. AFM was performed in liquid non-contact mode using a Park XE7 instrument and a cantilever with a spring constant of 2.8 N/m (FMR 10M, Park Systems).

10. Zeta Potential. Zeta potential was measured using a Malvern Zetasizer. PBA-MDP solutions at a concentration of 0.2% (w/v) were prepared in pH 7.4 HEPES buffer at glucose concentrations of 0, 25, 50, 100, and 200 mg/dL. COOH-MPD and OH-MDP were prepared the same as PBA-MDP at a concentration of 0.2% (w/v) and a glucose concentration of 0 mg/dL. For all samples, an 800 µL sample was added into a clear folded cuvette and evaluated by using the Huckel model at 25°C. Each sample was prepared and measured in triplicate.

11. Thioflavin T (ThT) assay. PBA-MDP was dissolved in DI water at a concentration of 0.4% (w/v) and adjusted to pH 7.4 by 0.1 M NaOH. An aliquot of 97 µL of the peptide solution was mixed with 97 µL of 2x HEPES buffer (pH 7.4, 20 mM HEPES and 280mM NaCl), 2 µL of a 10 mM ThT stock solution, and 2 µL of HEPES buffer containing 0 or 100,000 mg/dL glucose, for a final glucose concentration of 0 or 100 mg/dL, respectively. Fluorescence intensity was serially measured on a Tecan M200 microplate reader at excitation of 485 nm and emission of 528 nm with 5 min intervals. After incubating for 4 h, 2 µL of 101,000 mg/dL glucose in 1x HEPES buffer was added into the 0 mg/dL glucose sample to rapidly raise its final glucose concentration to 100 mg/dL. For the sample initially prepared at 100 mg/dL glucose sample, 2 µL of 1x HEPES buffer was added. Fluorescence intensity was recorded every 5 min for another 36 h. A background of ThT in pH 7.4 HEPES buffer was subtracted from all spectra.

12. Rheological Characterization. To evaluate the mechanical properties of PBA-MDP hydrogels, dynamic oscillatory rheology was performed on a TA Instruments Discovery HR-2 rheometer fitted with a Peltier stage using a parallel plate geometry with a diameter of 25 mm. Samples at 1.5% (w/v) were prepared as described above at glucose concentrations of 0, 25, 50, 100, and 200 mg/dL and incubated for 45 min before the measurement. An amplitude sweep was

performed to determine the linear viscoelastic range. Then a frequency sweep was performed at a constant strain (1% strain). To evaluate the time course of gelation, a time sweep was performed immediately after sample preparation (1% strain, 5 rad/s). A step-strain cycling study was also performed on 1.5% (w/v) PBA-MDP hydrogels prepared at 100 mg/dL glucose, cycling between 1% strain for 2 min and 100% strain for 30 s at an angular frequency of 5 rad/s. To assess shear-thinning, PBA-MDPs prepared at glucose concentrations of 0 and 100 mg/dL were studied under steady shear flow over a shear rate range of 0.001 to 10 s⁻¹.

2.13 In vitro Glucagon Release. PBA-MDP hydrogels (1.5% w/v) were first prepared at a glucose concentration of 100 mg/dL, as described above. Mixed into each 50 μL was added a pre-formed complex of 0.1 mg MCA-dasiglucagon and 0.05 mg protamine. Hydrogels were incubated for 45 min after preparation in 6-well plates, after which 2 mL of pH 7.4 HEPES buffer that contained 0, 25, 50, 100, and 200 mg/dL glucose was added. As a control, COOH-MDP was prepared, loaded with the MCA-dasiglucagon and protamine complex, and tested for release in a glucose-free buffer. At each time point, a 20 μL solution was taken and diluted 10 times for fluorescence analysis (Ex: 322 nm, Em: 398 nm). The MCA-dasiglucagon concentration of each sample was determined using a standard curve. After the measurement, 20 μL of fresh buffer containing the corresponding glucose concentration was added to maintain constant bulk buffer volume.

2.14 In vivo hypoglycemia protection. Using a previously established hypoglycemia mouse model,^[1] the prophylactic (preventative) use of this material was explored for its ability to reduce the severity of a sudden hypoglycemic onset. Briefly, male C57BL6/J mice, aged 8 weeks, were induced diabetic by streptozotocin (STZ) dosed at 150 mg/kg i.p.. Once non-fasted blood glucose (BG) levels were 600+ mg/dL, 7-8 days after STZ treatment, the study was initiated. After fasting for 8 h, mice with BG > 450 mg/dL were dosed with 0.5 IU/kg basal *insulin detemir* (*Levemir*, *Novo Nordisk*) via subcutaneous (s.c.) injection in a total volume of ~100 μL. After 4 h BG levels were corrected to within a normal range (~180 mg/dL) and mice were randomly divided into 4 groups (n=9-10 per group) and treated with buffer, dasiglucagon (10 μg), PBA-MDP hydrogel loaded with 10 μg dasiglucagon, or COOH-MDP hydrogel loaded with 10 μg dasiglucagon in 100 μL total volume injected s.c.. BG levels were monitored after the treatment (t = 0 min). To trigger hypoglycemia, AOF recombinant human insulin (Gibco) was

administered 2 h following treatment i.p. at a dose of ~3 IU/kg in saline. BG levels were monitored for another 4 h. Throughout the experiment, mice exhibiting “high” readings were noted with a BG value of 600 mg/dL, while “low” readings were noted as a BG value of 20 mg/dL and indicated as dead. These studies were detailed in a protocol approved by the University of Notre Dame Animal Care and Use Committee (Assurance of Compliance #A3093-01) and adhered to all relevant Institutional, State, and Federal guidelines.

2.15 Statistical Analysis. For each experiment, data was plotted and where appropriate, statistical analysis was performed using GraphPad Prism (V9.5.1). For *in vitro* experiments mean \pm SD is shown, while for *in vivo* experiments mean \pm SEM is shown, customary for *in vivo* studies. Where noted, statistical comparisons between groups were performed using a Student’s t-test (including using the using the Holm-Šídák method to correct for multiple comparisons) while studies comparing averages between groups used a one-way analysis of variance (ANOVA) with a Bonferroni multiple comparisons *post-hoc* test. The figure captions in the main text note sample sizes, error presentation format, and statistical testing, where appropriate.

Supplementary Data

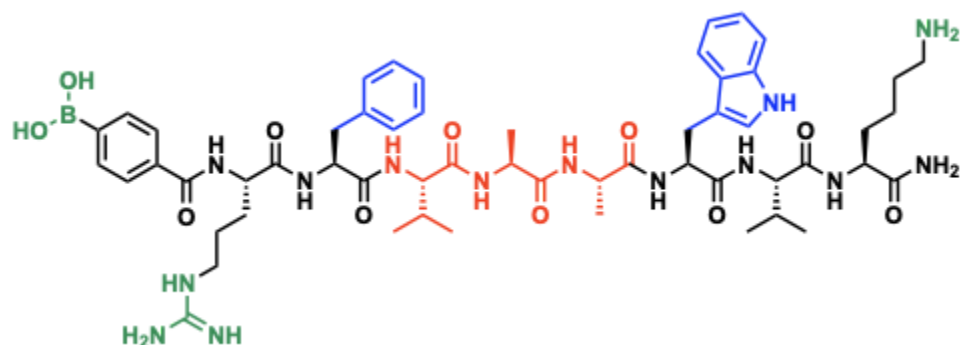


Figure S1: PBA-MDP Chemical Structure

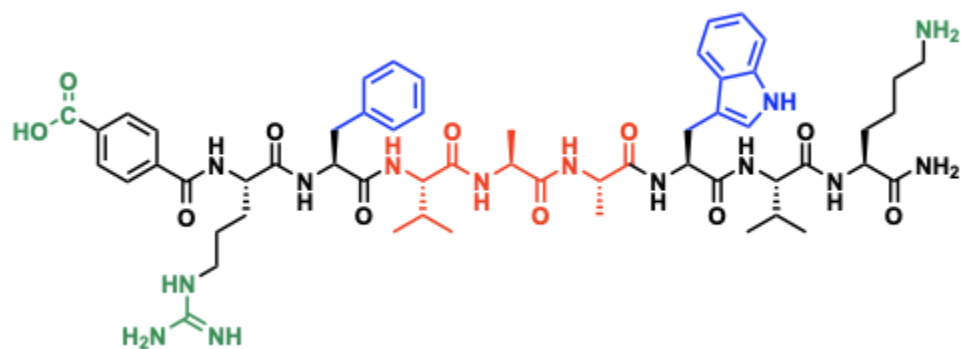


Figure S2: COOH-MDP Chemical Structure

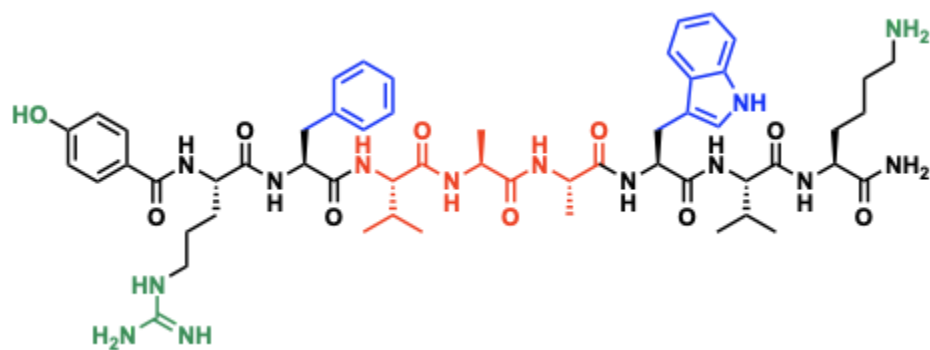


Figure S3: OH-MDP Chemical Structure

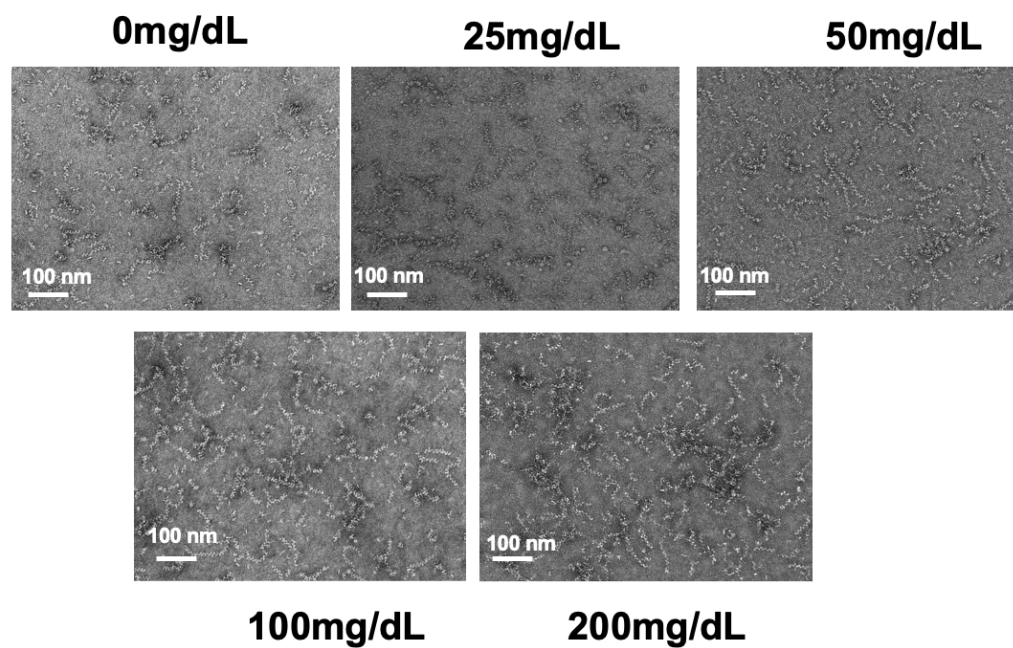


Figure S4: TEM analysis of PBA-MDP over a range of glucose concentrations.

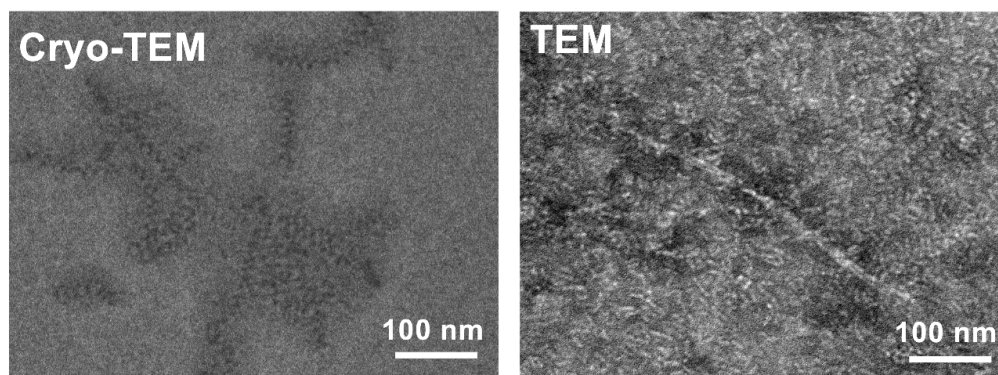


Figure S5: TEM analysis of COOH-MDP

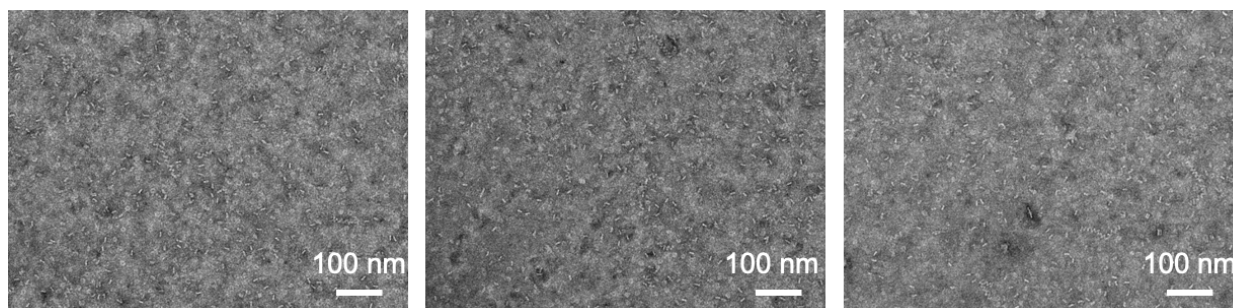


Figure S6: TEM analysis of OH-MDP

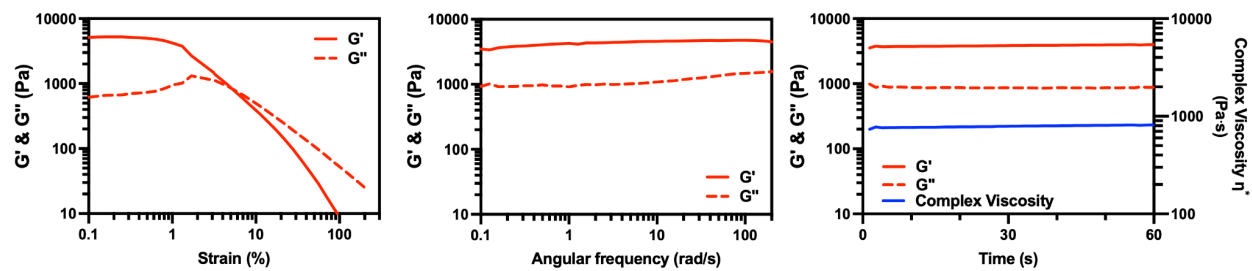


Figure S7: Rheology of COOH-MDP

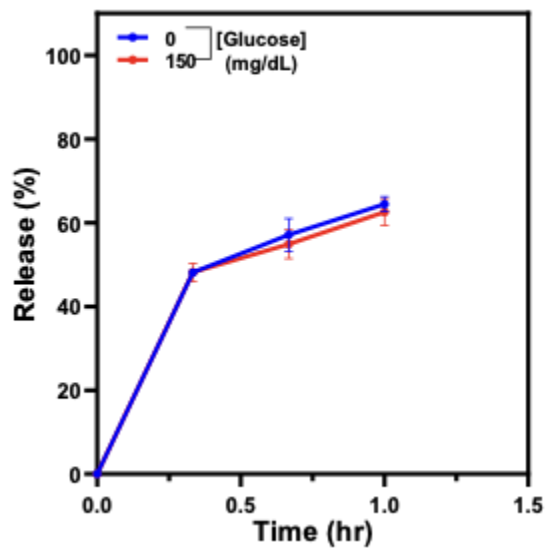


Figure S8: Release profile of MCA-dasiglucagon alone

Online Supporting Information

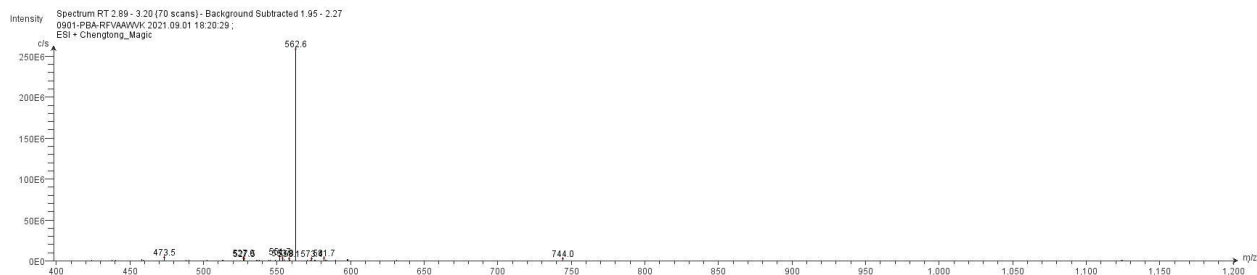


Figure S9: ESI-MS (positive mode) of PBA-RFVAAWVK. Calculated 1122.6 [M], observed 562.6 [M+2H]²⁺.

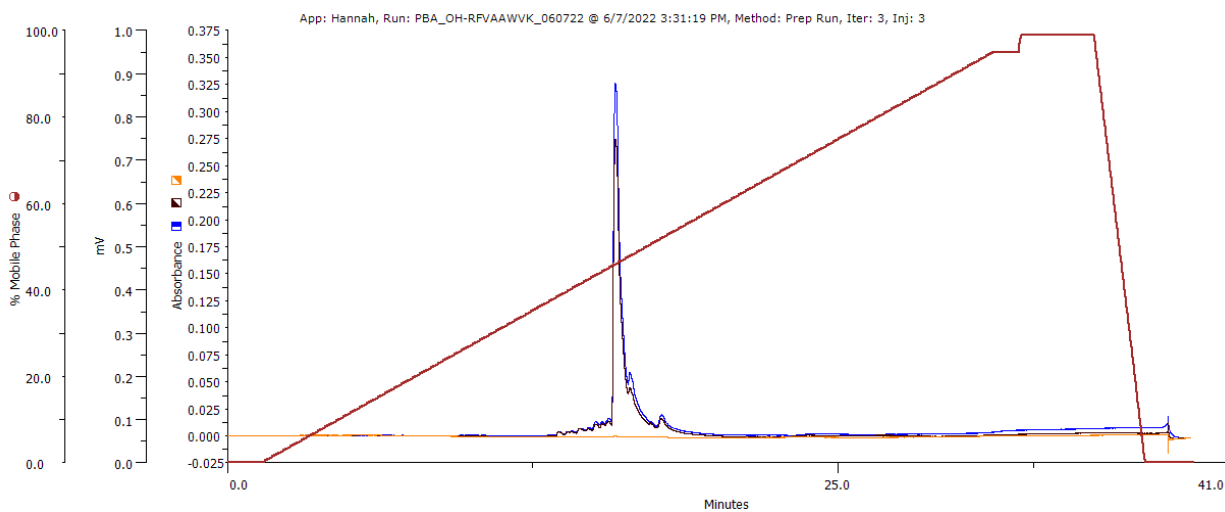


Figure S10: Analytical HPLC of PBA-RFVAAWVK with UV absorbance monitored at 220, 260, 280, and 350nm.

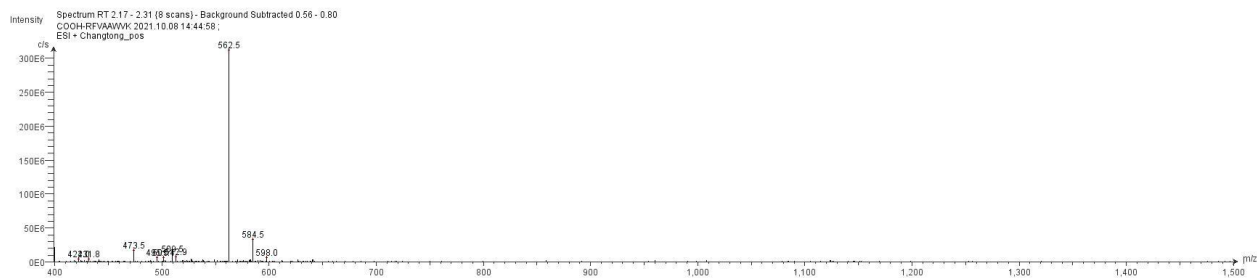


Figure S11: ESI-MS (positive mode) of COOH-RFVAAWVK. Calculated 1122.6 [M], observed 562.5 [M+2H]²⁺.

Online Supporting Information

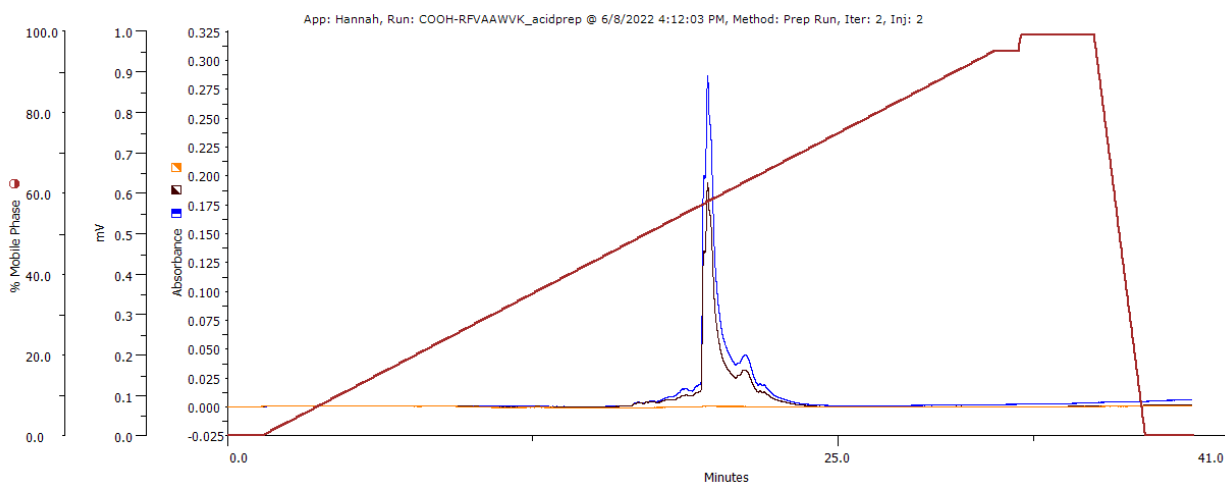


Figure S12: Analytical HPLC of COOH-RFVAAWVK with UV absorbance monitored at 220, 260, 280, and 350nm.

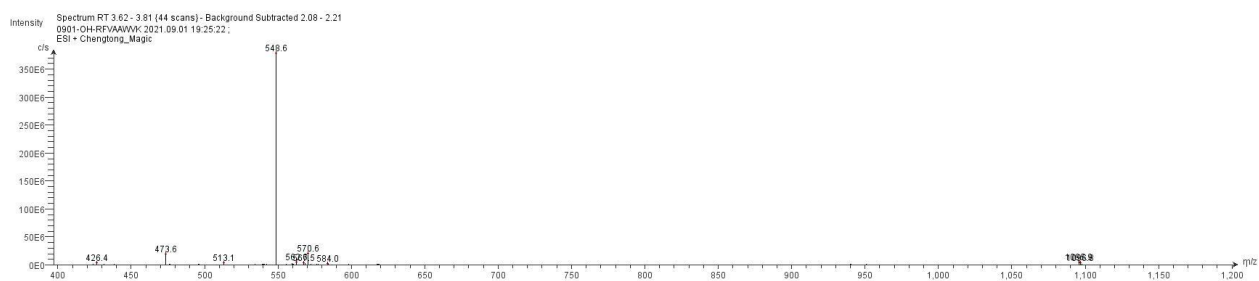


Figure S13: ESI-MS (positive mode) of OH-RFVAAWVK. Calculated 1094.6 [M], observed 548.6 [M+2H]²⁺.

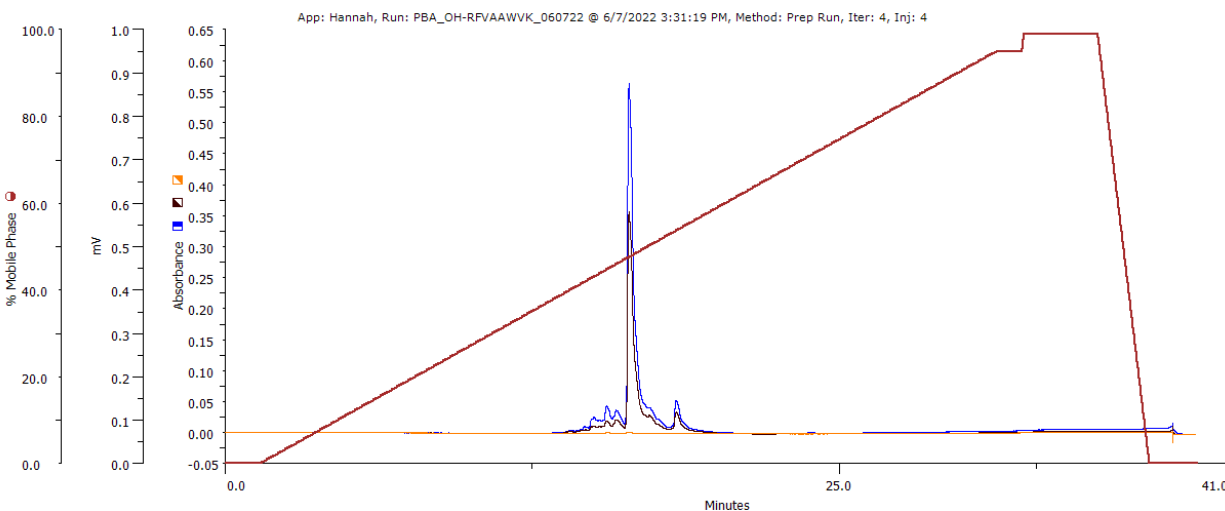
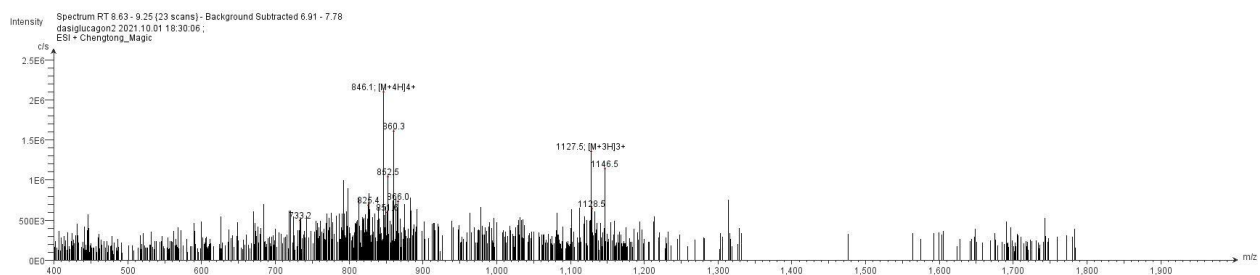


Figure S14: Analytical HPLC of OH-RFVAAWVK with UV absorbance monitored at 220, 260, 280, and 350nm.

Online Supporting Information



072921_dasiglucagon2 2021.07.29 17:21:39

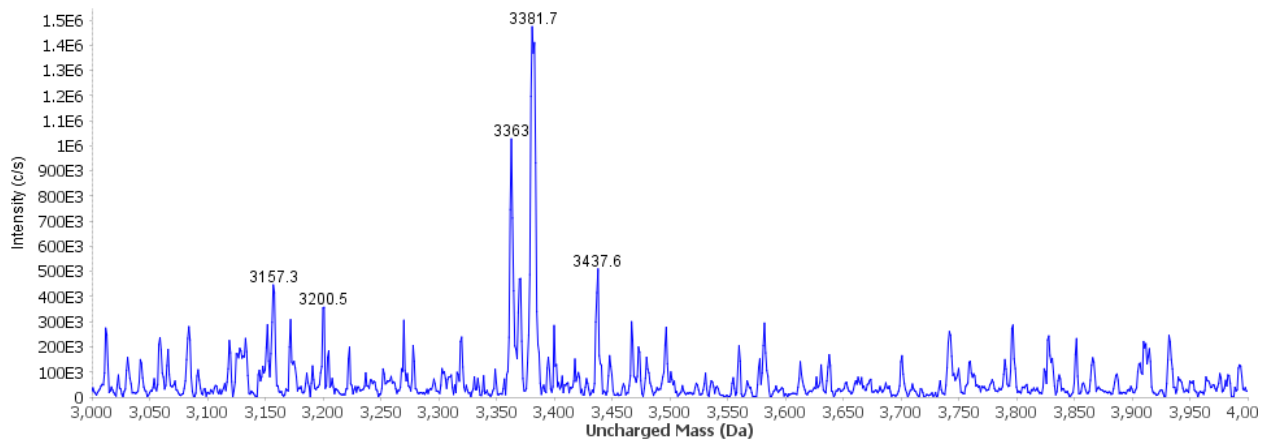


Figure S15: (top) ESI-MS of dasiglucagon (positive mode). Calculated 3381.6 [M], observed 1127.5 [M+3H]³⁺, 846.1 [M+4H]⁴⁺; (b) Deconvoluted ESI-MS spectra (uncharged).

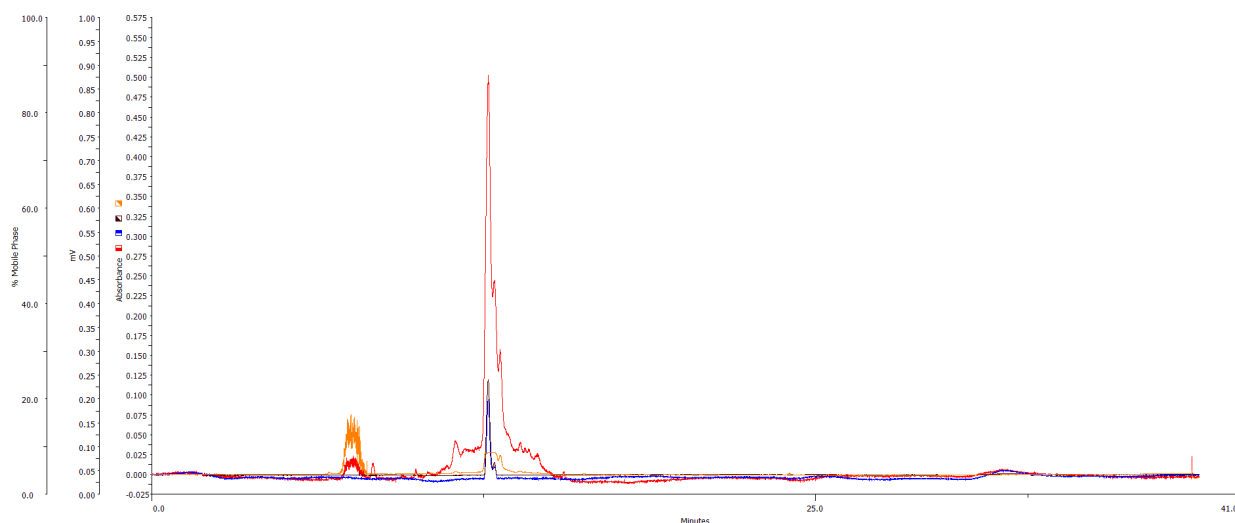


Figure S16: Analytical HPLC of dasiglucagon with UV absorbance monitored at 220, 260, 280, and 350nm.

References:

- [1] S. Yu, S. Xian, Z. Ye, I. Pramudya, M. J. Webber, *J. Am. Chem. Soc.* **2021**, *143*, 12578.
- [2] J. Ilavsky, P. R. Jemian, *J. Appl. Crystallogr.* **2009**, *42*, 347.
- [3] D. V. Lebedev, D. M. Baitin, A. K. Islamov, A. I. Kuklin, V. K. Shalguev, V. A. Lanzov, V. V. Isaev-Ivanov, *FEBS Lett.* **2003**, *537*, 182.
- [4] I. Breßler, J. Kohlbrecher, A. F. Thünemann, *J. Appl. Crystallogr.* **2015**, *48*, 1587.
- [5] Y. Wang, K. Kaur, S. J. Scannelli, R. Bitton, J. B. Matson, *J. Am. Chem. Soc.* **2018**, *140*, 14945.
- [6] A. Punjani, J. L. Rubinstein, D. J. Fleet, M. A. Brubaker, *Nat. Methods* **2017**, *14*, 290.
- [7] J. Jumper, R. Evans, A. Pritzel, T. Green, M. Figurnov, O. Ronneberger, K. Tunyasuvunakool, R. Bates, A. Židek, A. Potapenko, A. Bridgland, C. Meyer, S. A. A. Kohl, A. J. Ballard, A. Cowie, B. Romera-Paredes, S. Nikolov, R. Jain, J. Adler, T. Back, S. Petersen, D. Reiman, E. Clancy, M. Zielinski, M. Steinegger, M. Pacholska, T. Berghammer, S. Bodenstein, D. Silver, O. Vinyals, A. W. Senior, K. Kavukcuoglu, P. Kohli, D. Hassabis, *Nature* **2021**, *596*, 583.
- [8] P. Emsley, K. Cowtan, *Acta Crystallogr. D Biol. Crystallogr.* **2004**, *60*, 2126.